SPECTROMETER-DRIVEN SPECTRAL PARTITIONING FOR HYPERSPECTRAL IMAGE CLASSIFICATION

Jun Li[1], *Yi Liu*[2], *Antonio Plaza*[2], *Peijun Du*[3] *and Mahdi Khodadadzadeh*[2]

[1]School of Geography and Planning, Sun Yat-sen University, Guangzhou, P. R. China.
[2]Hyperspectral Computing Laboratory, Department of Technology of Computers and Communications, Escuela Politécnica, University of Extremadura, Cáceres, E-10071, Spain.
[3]Key Laboratory for Satellite Mapping Technology and Applications of State Administration of Surveying, Mapping, and Geoinformation of China, Nanjing University, Nanjing 210023, China.

ABSTRACT

Classification is an important and widely used technique for remotely sensed hyperspectral data interpretation. Although most techniques developed for classification assume that the spectral signatures provided by an imaging spectrometer can be interpreted as a unique and continuous signal, in practice this signal may be obtained after the combined individual responses from several different spectrometers. For instance, the Airborne Visible Infra-Red Imaging Spectrometer (AVIRIS) system is in fact formed by four different spectrometers, covering the nominal spectral ranges of 400-700 nm, 700-1300 nm, 1300-1900 nm, and 1900–2500 nm, respectively. In this work, we propose a new classification strategy which takes into account the physical design of the imaging spectrometer system for partitioning the spectral bands collected by each spectrometer, and resampling them into different groups or partitions. The final classification result is obtained as a combination of the results obtained from each individual partition. This concept is illustrated in this work using AVIRIS data, and our experimental results indicate that the proposed strategy provides advantages in terms of classification accuracy, in particular, when very limited training samples are available.

Index Terms— Spectrometer-driven classification, partitioning, clustering, AVIRIS.

1. INTRODUCTION

In the last two decades, imaging spectroscopy (also called hyperspectral remote sensing) has experienced significant developments [1]. Currently, many sensors onboard airborne and spaceborne platforms are available, and these instruments keep collecting data from different locations over the Earth [2]. Hyperspectral image classification has been a very important topic of research for interpreting hyperspectral data [3], in which the main challenges have been given by the high dimensionality of the data and the limited number of training samples generally available [4]. A main assumption of most classification techniques is that the spectral signatures provided by an imaging spectrometer system for a given pixel can be considered as a unique and continuous signal.

However, in practice this signal may be obtained after the combined individual responses from several different spectrometers. For instance, the Airborne Visible Infra-Red Imaging Spectrometer (AVIRIS) system [5] is in fact formed by four different spectrometers, covering the nominal spectral ranges of 400-700 nm, 700-1300 nm, 1300-1900 nm, and 1900–2500 nm, respectively. These four spectrometers, called A, B, C and D respectively, have different characteristics. For instance, in the D spectrometer a carefully specified linear variable blocking filter is used to limit the wavelengths of light for each element in the detector array. This specialized filter reduces the noise arising from photons emitted by the spectrometer in the 1900-2500 nm spectral range. For the A spectrometer, a 32-element silicon detector array with a blue enhanced response is used. The B, C and D spectrometers each have 64-element arrays instead.

Given the fact that different spectrometers have different characteristics, our speculation in this work is that the conventional interpretation that the spectral signatures can be interpreted as unique and distinct signals may not hold in all cases, and that the use of a spectrometer-driven partitioning prior to classification may lead to improved hyperspectral data interpretation results. Specifically, in this work we propose a new spectrometer-driven classification strategy that considers the differences between the individual spectrometers in the classification step. An important consideration of our approach is that, as the dimensionality of each spectrometer signal is much smaller than the whole spectral signal, it allows for the design of a classification system that is efficient in scenarios in which limited training samples are available *a priori*. Here we illustrate the concept using AVIRIS data. In order to handle the existing correlation between spectral bands, we use a band partitioning approach driven by the four different spectrometers of AVIRIS, as the hyperspectral bands captured by each of them exhibit similar characteristics.

The remainder of this paper is organized as follows. In section 2, we first introduce the proposed spectrometer-driven spectral partitioning strategy. Then, we present our classification system based on the recently developed subspace-based multinomial logistic regression (MLRsub), an efficient technique able to deal with very limited training samples [6]. Experimental results with AVIRIS data are given in section 3. Finally, section 4 concludes this work with some remarks.

2. SPECTROMETER-DRIVEN PARTITIONING AND HYPERSPECTRAL IMAGE CLASSIFICATION

In this section, we first introduce a spectrometer-driven spectral partitioning method and then present a strategy used for classification of AVIRIS hyperspectral data based on the MLRsub classifier. In the spectrometer subsystem of AVIRIS, light from each of the optical fibers enters a different spectrometer covering a portion of the AVIRIS spectral range. The four spectrometers cover the nominal

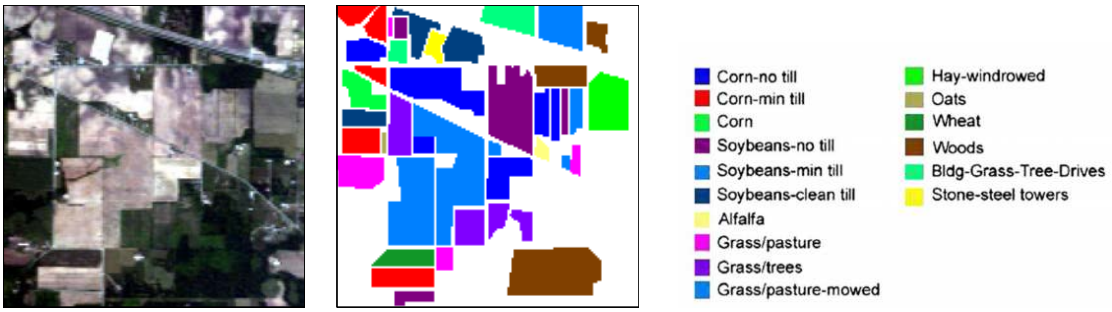

(a) False color representation (b) Available reference classes

Fig. 1. AVIRIS Indian Pines data set.

spectral ranges of 400–700 nm, 700–1300 nm, 1300–1900 nm, and 1900–2500 nm, respectively. If we take the popular AVIRIS Indian Pines data set[1], the corresponding band intervals are [1,31], [32,94], [95,157] and [158,220], respectively. This scene, displayed in Fig. 1(a), comprises 145 $\times$ 145 pixels and was recorded over Northwestern Indiana in June of 1992. As shown by Fig. 1(b), a total of 10366 pixels are available in the labeled ground-truth, including 16 mutually exclusive classes. Although some of the bands are considered to be corrupted by water absorption and noise, we will use all of them since the MLRsub classifier considered in this work has the capability to manage noise and mixtures by projecting the data to the class indexed subspaces. Although some of the bands are considered to be corrupted by water absorption features and noise, we will use all of them since the MLRsub classifier considered in this work has the capability to manage noise and mixtures by projecting the data to the class indexed subspaces.

2.1. Spectrometer-Driven Spectral Partitioning

In this subsection we describe the spectrometer-driven spectral partitioning strategy and use the AVIRIS Indian Pines data for illustrative purposes. Since in this case the spectral vectors are collected by four spectrometers, the band continuity for each spectrometer is expected to be quite high. Fig. 2 shows the spectral clustering results obtained from the adaptive affinity propagation (AAP) approach [7], which uses the coefficient of correlation as the measurement of similarity. Fig. 2 illustrates that there are high spectral similarities among continuous bands collected by each of the four spectrometers. Based on this observation, in this work we perform band partitioning based on the four spectrometers to resample the spectral bands to different groups (or partitions), such as to exploit the spectral information by reducing the spectral similarities and increasing the partition distance.

The proposed spectrometer-based spectral partitioning approach is different from conventional spectral clustering approaches, which generally considers the spectral signatures as a whole. Therefore, based on the observed spectral correlations, we resample the bands into different partitions for each spectrometer. In this study, after resampling, we obtained a total of five partitions, each with 42 spectral bands. Now each pixel in the original hyperspectral image can be resampled by taking one spectral band from each one of the five partitions, so that we can obtain five different (subsampled) representations of the original pixel. In order to illustrate this concept, Fig. 3(a) shows the spectral signature of pixel at spatial location (100,100) in the the original AVIRIS Indian Pines data, while Fig. 3(b) presents the five subsampled spectral signatures for the same pixel obtained by using the five available partitions. As we can see in Fig. 3, the subsampled spectral signatures are very similar to the spectral signature, which means that the partitions are able to capture the spectral characteristics of whole spectral signature while reducing its dimensionality. On the other hand, the spectral signatures in the original image, although similar, have some differences across all the bands. Based on this property, the proposed strategy is able to exploit the different characteristics of the spectral signature in each of the considered partitions.

[1]https://engineering.purdue.edu/biehl/MultiSpec/hyperspectral.html

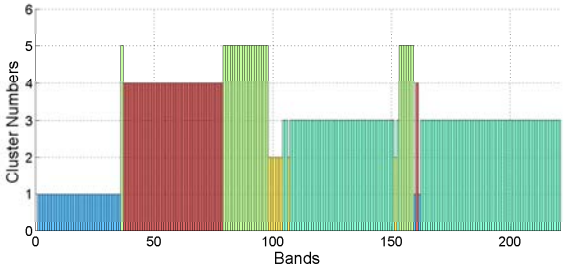

Fig. 2. Spectral clustering results based on adaptive affinity propagation (AAP) for the AVIRIS Pines Scene image.

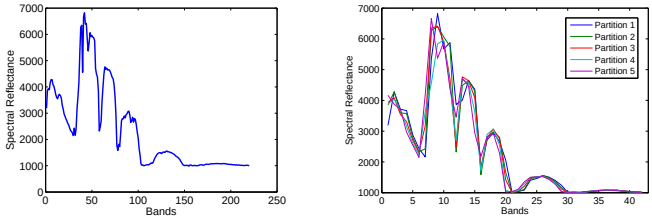

(a) Original spectral signature (b) Sub-sampled spectral signatures

Fig. 3. spectral signature of pixel at spatial location (100,100) in the the original AVIRIS Indian Pines data (a) and the five subsampled spectral signatures for the same pixel obtained by using the available partitions (b).

2.2. Hyperspectral Classification Using the MLRsub

Recently, the MLRsub method [6] has been specifically designed to address challenging hyperspectral classification problems. Specifically, in the MLRsub the classification of a pixel (with its associated

spectral vector in a given class) corresponds to the largest projection of that vector onto the class indexed subspaces. In this subsection, we highlight the decision rule adopted for fusing the individual classifications (obtained by the MLRsub) of the spectral signatures from the partitions that we obtained using the procedure described in the previous subsection. Let $\mathbf{p}_m(i)$ be the probabilities for a given pixel i and partition m. In this work, we use a simple strategy to combine the results obtained from all the partitions, as given below:

$$\hat{\mathbf{p}}(i) = \frac{1}{n}\sum_{m=1}^{n}\mathbf{p}_m(i), \quad (1)$$

where n is the number of partitions. Resulting from (1), the final class label of pixel i is determined as follows:

$$\hat{\text{class}}(i) = \arg\max_{k\in\{1,\ldots,K\}} \hat{p}^{(k)}(i), \quad (2)$$

where K is the number of classes, $\hat{p}^{(k)}(i)$ is the probability corresponding to class k for a given pixel i, and $\hat{\mathbf{p}}(i) = [\hat{p}^{(1)}(i), \ldots, \hat{p}^{(K)}(i)]$. It should be noted that, after obtaining the joint probability, we perform Markov random field (MRF)-based spatial regularization [8] to promote a classification solution with spatial smoothness, as indicated in [6].

3. EXPERIMENTAL RESULTS

This section describes our experimental results with the AVIRIS Indian Pines scene in Fig. 1. As mentioned in the previous section, after the spectral partitioning and resampling we obtain five partitions, each with 42 spectral bands. In order to analyze the impact of our spectrometer-driven partitioning framework on the classification of the scene, we first analyze the performance of the method as a function of the dimensionality of the estimated subspace by the MLRsub technique. Then, we analyze the sensitivity of the MLRsub to the number of training samples, thus addressing the two main issues in supervised classification of hyperspectral data (dimensionality and limited training samples). In all cases, we set the parameter β (which controls the degree of smoothness obtained after applying the MRF to the classification result obtained by the MLRsub) to $\beta = 2$, according to our previous studies [6], in which it was shown that appropriate results could be obtained with β in the range [0.5,4].

3.1. Impact of the Dimensionality of the Estimated Subspace

In this experiment, 10% of the 10366 pixels available in the ground truth image in Fig. 1(b) are used for training, while the remaining samples are used for testing. Fig. 4 shows the overall classification accuracies (OA) as a function of the dimensionality of the subspace, for both the original hyperspectral image [see Fig. 1(a)] and for the five partitions [see Fig. 1(b)]. It is remarkable that the results obtained for each partition are very close to the results obtained using the original image with all the spectral bands. Another important observation is that, for all the partitions, the optimal dimensionality was achieved in the interval [10, 15], as it was also the case for the original image. This means that working in the partition domain allows further possibilities to determine the optimal subspace dimensionality without losing accuracy in the estimation with regards to the case in which the original hyperspectral image was used. Since the estimation of the dimensionality of the subspace is an important aspect for the MLRsub algorithm, we can conclude that the algorithm performs similarly from this viewpoint in the original and in the partitioned domain.

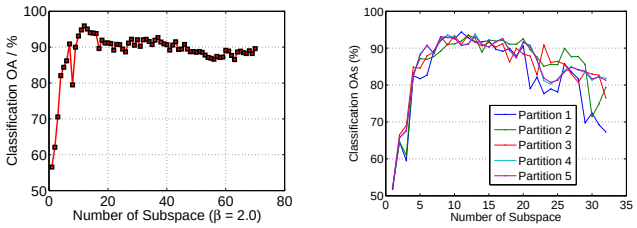

(a) Original data (b) Partitions

Fig. 4. Overall accuracies (OAs) obtained by the MLRsub method (followed by MRF postprocessing) as a function of the dimensionality of the subspace, for both the original image (a) and for the five partitions (b).

3.2. Impact of the Number of Training Samples

In this experiment we evaluate the impact of the number of available training samples in the proposed spectrometer-driven partitioning approach, as compared to the case in which the full spectral information is used. For simplicity, we analyze the cases in which the dimensionality of the subspace used for the MLRsub classifier is 11 and 13 (the two best cases in Fig. 4. For that purpose, Fig. 5(a) shows the OAs (as a function of the number of training samples used per class) obtained when applying the MLRsub with and without the proposed partitioning strategy to the AVIRIS Indian Pines scene, considering that the dimensionality of the subspace is 11. Similarly, Fig. 5(b) shows the OAs (as a function of the number of training samples used per class) obtained when applying the MLRsub with and without the proposed partitioning strategy to the AVIRIS Indian Pines scene, considering that the dimensionality of the subspace is now 13. The color areas around each plot in Fig. 5 represent the standard deviation.

Several conclusions can be obtained from Fig. 5. First and foremost, the proposed approach with spectral partitioning outperforms the classic MLRsub configuration when limited training samples are available. For instance, the proposed approach obtained an OA greater than 85% by using only 20 labeled samples per class, increasing significantly the OA obtained by the original strategy in the same conditions. Furthermore, it is remarkable that the standard deviations obtained by the proposed partitioning-based approach are significantly smaller than those achieved by the MLRsub with the original hyperspectral image. Finally it is also noticeable that, after a given number of training samples (i.e., 60 samples per class in our experiment), the results obtained with the full original image are better than those obtained using th proposed partitioning approach. This is due to the fact that the dimensionality of the partitions and the class boundaries are well-defined after a sufficient set of training samples are available.

Finally, Fig. 6 shows the obtained classification maps for the AVIRIS Indian Pines by using 20 labeled samples per class under an optimal setting of dimensionality of the subspace. In this particular case, the proposed approach obtained an OA of 87.83% which is about 20% higher than the OA obtained after applying the MLRsub (plus the MRF regularization) to the full original hyperspectral image. We can therefore conclude that the proposed spectrometer-driven partitioning approach can provide good classification results in the presence of limited training samples.

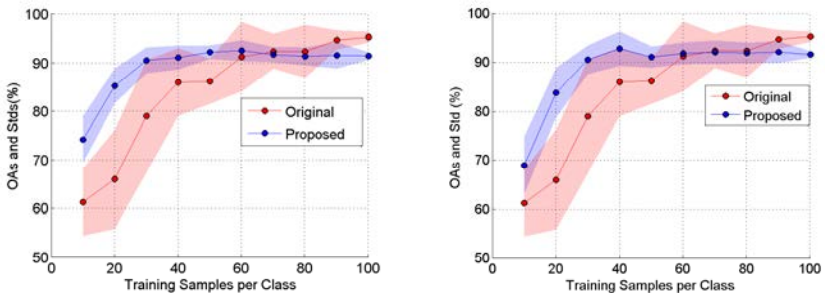

(a) Dimensionality of the subspace: 11 (b) Dimensionality of the subspace: 13

Fig. 5. Overall accuracies (as a function of the number of training samples used per class) obtained when applying the MLRsub, with and without the proposed partitioning strategy, to the AVIRIS Indian Pines scene, considering that the dimensionality of the subspace is 11 (a) and 13 (b). The color areas around each plot represent the standard deviation around the mean.

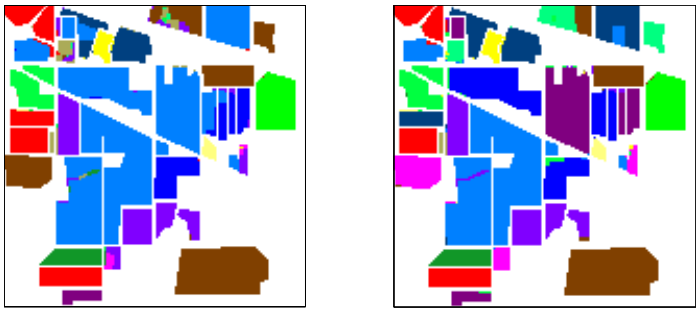

(a) Classification map using the original data (b) Classification map using the proposed approach

Fig. 6. Classification maps obtained using 20 training samples per class.

4. CONCLUSIONS AND FUTURE LINES

In this work, we have developed a new spectrometer-driven based technique for hyperspectral image partitioning and classification. The proposed approach takes into account the physical design of the imaging spectrometer system for partitioning the spectral bands collected by each spectrometer, and resampling them into different groups or partitions. Instead of considering the spectral signatures as unique continuous signals, here we consider each spectral signature as a signal that is contributed from different instrument sources, and partition the data accordingly prior to conducting the classifications step. We have evaluated the methodology by using the AVIRIS instrument. Our experimental results indicate that the proposed strategy can exploit the information contained in each spectrometer in order to improve the classification results using limited training samples. In the future, we will use other imaging spectrometers and classification techniques in order to analyze the generality of the presented approach. We are also planning on using different numbers of bands for each partition (in the present configuration all partitions have the same number of bands) in order to better model the contributions from each spectrometer.

References

[1] A. Plaza, J.A. Benediktsson, J.W. Boardman, J. Brazile, L. Bruzzone, G. Camps-Valls, J. Chanussot, M. Fauvel, P. Gamba, A. Gualtieri, et al., "Recent advances in techniques for hyperspectral image processing," *Remote Sensing of Environment*, vol. 113, pp. S110–S122, 2009.

[2] J. Bioucas-Dias, A. Plaza, G. Camps-Valls, P. Scheunders, N. Nasrabadi, and J. Chanussot, "Hyperspectral remote sensing data analysis and future challenges," *IEEE Geoscience and Remote Sensing Magazine*, vol. 1, pp. 6–36, 2013.

[3] M. Fauvel, Y. Tarabalka, J. A. Benediktsson, J. Chanussot, and J. C. Tilton, "Advances in spectral-spatial classification of hyperspectral images," *Proceedings of the IEEE*, vol. 101, no. 3, pp. 652–675, 2013.

[4] D. A. Landgrebe, *Signal Theory Methods in Multispectral Remote Sensing*, John Wiley & Sons: New York, 2003.

[5] R. O. Green, M. L. Eastwood, C. M. Sarture, T. G. Chrien, M. Aronsson, B. J. Chippendale, J. A. Faust, B. E. Pavri, C. J. Chovit, M. Solis, et al., "Imaging spectroscopy and the airborne visible/infrared imaging spectrometer (AVIRIS)," *Remote Sensing of Environment*, vol. 65, no. 3, pp. 227–248, 1998.

[6] J. Li, J. Bioucas-Dias, and A. Plaza, "Spectral-spatial hyperspectral image segmentation using subspace multinomial logistic regression and Markov random fields," *IEEE Trans. Geosci. and Remote Sens.*, vol. 50, no. 3, pp. 809–823, 2012.

[7] Hongjun Su, Yehua Sheng, Peijun Du, and Kui Liu, "Adaptive affinity propagation with spectral angle mapper for semi-supervised hyperspectral band selection," *Appl. Opt.*, vol. 51, no. 14, pp. 2656–2663, May 2012.

[8] Stan Z. Li, *Markov Random Field Modeling in Image Analysis*, Springer-Verlag New York, Inc., second edition, 2001.